A molecular dynamics study of the structural change differences between Au_{225} and Au_{369} clusters on MgO surfaces at low temperature*

Zhang Lin(张 林)[a)†], Wang Shao-Qing(王绍青)[b)], and Chen Nan-Xian(陈难先)[c)]

[a)] *Institute of Materials Physics and Chemistry, College of Science, Northeastern University, Shenyang* 110004, *China*

[b)] *Shenyang National Laboratory for Materials Science, Institute of Metal Research, Chinese Academy of Sciences, Shenyang* 110016, *China*

[c)] *Physics of Department, Tsinghua University, Beijing* 100084, *China*

(Received 23 July 2011; revised manuscript received 17 October 2011)

The differences in structural change between Au_{225} and Au_{369} clusters with their (111) facets supported on MgO(100) surfaces at 5 K are studied by using molecular-dynamics simulations with the atomic interchange potentials of the Au/MgO interface. The parameters are obtained from the *ab initio* energies using the Chen–Möbius inversion method. Analyses of the pair distribution functions show that the two Au clusters use different deformation processes to adjust the distances between the interface atoms, owing to the misfit between the atom distances among the clusters and the substrates. The local structural changes are identified by atomic density profiles.

Keywords: interfaces, nanostructures, computer modelling and simulation, molecular dynamics

PACS: 36.40.Ei, 31.15.xv, 07.05.Tp, 64.60.an **DOI:** 10.1088/1674-1056/21/3/033601

1. Introduction

An enormous surge of interest has recently arisen in investigations of coinage metals including gold, silver and copper in the form of nanoparticles with crystalline characteristics supported on metal-oxide substrates at low temperatures. The cluster–support interaction is therefore a crucial issue when rationalizing observations on such systems and using this knowledge to manipulate matter on the nanometer length scale for applications in heterogeneous catalysis, bioelectrocatalysis, labeling, photonics, nanocircuits, magnetic devices and mechanically high-strength granular materials.[1,2] However, it is usually difficult to obtain comprehensive information about metal/oxide interfaces from experiments, because their properties are affected by many uncontrollable factors under the *in-situ* experimental conditions. On the other hand, theoretical approaches such as molecular dynamics (MD), quantum chemistry and computer graphics enable us to separate those factors and furnish a complementary means for expanding our understanding of the complexes of nanoscale clusters with oxide support.[3−8] In the investigation of the interaction between metals and metal oxides using the first-principles calculations, the absorption properties of Ag clusters on SrTiO3(001) and CdS(0001) surfaces were studied,[9,10] and the atomic Cu adsorption on defect-free SrTiO3(001) surfaces was also investigated.[11] Nevertheless, the sophisticated first-principles approach cannot be implemented on large supported nanoparticles owing to the prohibitive computational expense.[12−15] Thus, the molecular dynamics simulation is a common optimal approach for exploring the local structural rearrangements at the atomic level.[16−25] Among the coinage clusters, gold nanoparticle catalysts are used mainly in selective oxidation reactions and a broad range of organic transformations besides possessing hydrogenation activity.[26] The Au clusters containing tens of atoms have been extensively studied.[27] However, the microscopic evolutions in those small systems containing hundreds of atoms have not yet been fully understood. Those clusters usually have spherical shapes

*Project supported by the State Key Development Program for Basic Research of China (Grant No. 2011CB606403), the Fundamental Research Foundations for the Central Universities, China (Grant No. N90405001), and the National Natural Science Foundation of China (Grant No. 51171044).

†Corresponding author. E-mail: zhanglin@imp.neu.edu.cn

© 2012 Chinese Physical Society and IOP Publishing Ltd

covered by (100)- and (111)-like facets. In the previous work, the structural changes of Au clusters containing 603 and 675 atoms with their (100) facets supported by MgO(010) surfaces were investigated.[28] To the best of our knowledge, there are still few studies on the structural changes of the Au clusters with their (111) facets supported by the MgO(010) surfaces, while the defect-free MgO(010) surface often serves as a model because of its simplicity, non-polarity and low reactivity.

This paper aims to explore the structural change differences between the Au clusters containing 225 and 369 atoms with their (111) facets over the MgO(010) surface at a temperature of 5 K using MD simulations. How the structural change is accompanied by atomic packing is demonstrated by pair distribution functions (PDFs). Here, regions with multilayer structures of studied clusters are determined by atomic density profile calculations.

2. Methods

In the Au/MgO system, there are three kinds of interactions: the Au–Au interaction $\Phi_{\text{Au–Au}}$ on the Au cluster side, the oxide–oxide interactions $\Phi_{\text{Mg–Mg}}$, $\Phi_{\text{Mg–O}}$ and $\Phi_{\text{O–O}}$ on the oxide side, and the Au–oxide interactions $\Phi_{\text{Au–O}}$ and $\Phi_{\text{Au–Mg}}$ across the interface. The Au–Au interactions are described by short-range potentials. They are extracted from the *ab initio* cohesive energies using the Chen–Möbius inversion method.[29,30] The Rahman–Stillinger–Lemberg potential used throughout the calculation is given by

$$\Phi = D_0\,\mathrm{e}^{v(1-r/R_0)} + \frac{a_1}{1+\mathrm{e}^{b_1(r-c_1)}} + \frac{a_2}{1+\mathrm{e}^{b_2(r-c_2)}} + \frac{a_3}{1+\mathrm{e}^{b_3(r-c_3)}}, \quad (1)$$

where D_0, v, R_0, a_1, a_2, a_3, b_1, b_2, b_3, c_1, c_2 and c_3 are potential parameters, which can be found in Refs. [29] and [30], and r is the distance between the atoms. As MgO is an ion crystal, the interaction is composed of two parts: the long-range part, which is the Coulomb interaction and is determined by an effective charge Q_{eff} of $2e$

$$\Phi^{\text{Coul}}_{\text{Mg–Mg}} = \Phi^{\text{Coul}}_{\text{O–O}} = -\Phi^{\text{Coul}}_{\text{Mg–O}} = \frac{Q^2_{\text{eff}}}{4\pi\varepsilon_0 r}, \quad (2)$$

and the short-range part, which is in the Morse or exp-repulsive form, with the parameters presented in Refs. [29] and [30].

Initially, we constructed a $12a_0\times40a_0\times12a_0$ bulk MgO containing 46080 atoms, where $12a_0\times40a_0\times12a_0$ is the volume of the MD simulation cell, and lattice constant a_0 is 0.4216 nm. A crystal fragment containing 9792 atoms with double-free surfaces is extracted from this constructed bulk crystal, and used as the support in the simulations. Then, Au clusters containing 225 atoms and 369 atoms are put on the MgO surfaces with their (111) facets supported by the MgO(010) surfaces. The two Au clusters have face centered cubic (FCC) structures and are covered by (100)- and (111)-like facets. Periodic boundary conditions are used in the simulations. Figures 1(a) and 1(b) show the PDFs of the Au_{225} and the Au_{369} clusters and their initial structures at 5 K. As shown in these figures, the two clusters present the FCC structural characteristics with ABC packing ordering along the $\langle 1\bar{1}2\rangle(111)$ direction. For the Au_{225} cluster, the bottom contacting the MgO surface is composed of three atoms, and for the Au_{369} cluster, it is composed of 18 atoms. The PDFs also prove that both clusters have typical FCC structures. The PDF shows one main peak with some other small peaks, and the main peak is far higher than the other peaks, which implies that most of the atom pairs are populated in the first peak. It should be noted that the first peak positions of the two PDFs are $0.685a_0$, corresponding to 0.289 nm, which is the distance between the nearest neighbors of gold atoms in the gold bulk.

In the calculations, each run takes 400000 time steps, and the atomic trajectories are recorded to study the structural properties of the simulated systems. A time step of 1.6 fs is used in the calculations. The temperature is kept constant by rescaling the atomic velocities at each time step. For calculating the structural changes of these clusters, the following values are determined:[31]

$$g_{Lg}(r) = \frac{V}{N}\left\langle \sum_{i\in Lg}\sum_{j\neq i\in Lg}\delta(\boldsymbol{r}-\boldsymbol{r}_{ij})\right\rangle, \quad (3)$$

$$\rho(y_i) = \langle N_i\rangle/N, \quad (4)$$

where $\langle\ \rangle$ denotes the average over the trajectory, $g_{Lg}(r)$ is the pair distribution function in layer Lg, V is the volume of the simulated MD cell, and N is the atom number in the cell. The density profile $\rho(y_i)$ is calculated by dividing the system into some layers and accumulating a histogram of the number, where $\langle N_i\rangle$ is the average number of atoms in layer i, and y_i is the center position of this layer along the y direction.

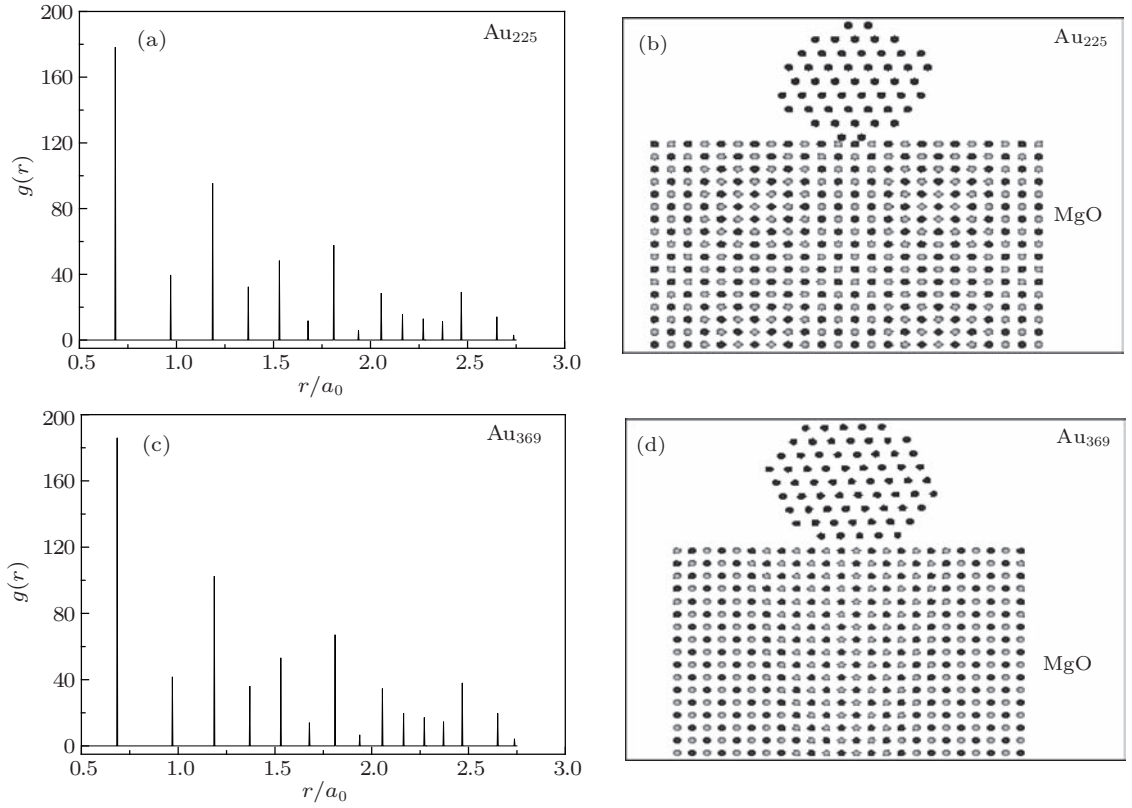


Fig. 1. PDFs ((a) and (c)) and initial structures ((b) and (d)) of the Au_{225} and Au_{369} clusters on MgO(010).

3. Results and discussion

To identify the differences in structural change between the two supported clusters, we plotted the time variations of the PDFs for the Au_{225} and the Au_{369} clusters, as well as their atomic configurations, in Figs. 2(a) and 2(b). For the Au_{225} cluster, at 0.024 ns, although the peak positions of its PDF are not changed compared with those of its initial form, as shown in Fig. 1(a), both the heights and the shapes of the peaks are obviously changed. This gives us an implication that the structural changes occur in the atomic configuration at this time, in which a few atoms of the Au_{225} cluster near the MgO(010) surface have left their initial positions. With the interaction time increasing, the structural changes become more apparent. At 0.032 ns, the PDF peak positions shift to the right, and the first peak position of the PDF is at $0.725a_0$, suggesting an increase of the distance among atoms. In addition, the first peak height of the PDF decreases, and the other peaks become very small, implying the occurrence of large deformation in this cluster, which can be observed in the atomic packing at this time. Then at 0.048 ns, as the first peak of the PDF becomes high and clear, the other peaks can apparently also be observed. As the interaction time increases, the PDF peak heights increase, and the atomic configuration becomes ordered, as shown in the right atomic packing. When the interaction time reaches 0.64 ns, the PDF presents one main peak and some small peaks similar to those of the initial structure. At this time, although the supported Au_{225} cluster has the FCC structure characteristic, as shown in its atomic configuration having the *ABC* packing order along the $\langle 1\bar{1}2\rangle(111)$ direction, this cluster has a shape that is different from its initial one, and more Au atoms contact the support surface.

For the Au_{369} cluster, in a short time the PDFs present similar change behaviors to those of the Au_{225} cluster. At 0.0216 ns, all the peaks in the PDF decrease compared with those of the initial structure. At 0.048 ns, except for the first and the third peaks, the other peaks become quite small, suggesting that the cluster undergoes an apparent deformation, which is proven to be in the atomic configuration at this time. Meanwhile, the distance between the atoms starts to increase. As the interaction between the Au_{369} cluster and the support surface proceeds, the atomic configuration shows that the deformation region becomes small, and after 0.072 ns, the cluster again has the FCC structure. Correspondingly, with an increase in

time the peak heights increase and the other small peaks become apparent. It can also be observed that the PDF peaks of the Au_{369} cluster are located at the same positions as those of the Au_{225} cluster, while the peak heights of the PDF for the Au_{369} cluster are apparently higher than those for the Au_{225} cluster, which is proof that the Au_{369} cluster has a different structure from the Au_{225} cluster when they are supported on the MgO(010) surfaces. The following atomic density profiles and the corresponding atomic packings are used to illustrate the detailed structural changes of the Au_{225} and the Au_{369} clusters during their interaction with the MgO surface, as shown in Figs. 3 and 4, respectively. The left parts of the two figures show the atomic density profiles of these two clusters at different times along the [010] direction of the MgO surface, where the peaks in the long lines represent the MgO substrate and the peaks in the short lines represent the Au clusters. The right parts show the atomic packings of the Au atoms in different layers numbered as 1–9 and determined by the short lines in the atomic density profiles along $\langle 1\bar{1}1\rangle$ of the clusters, where the atomic packings are recorded from the positions of the atoms at different times.

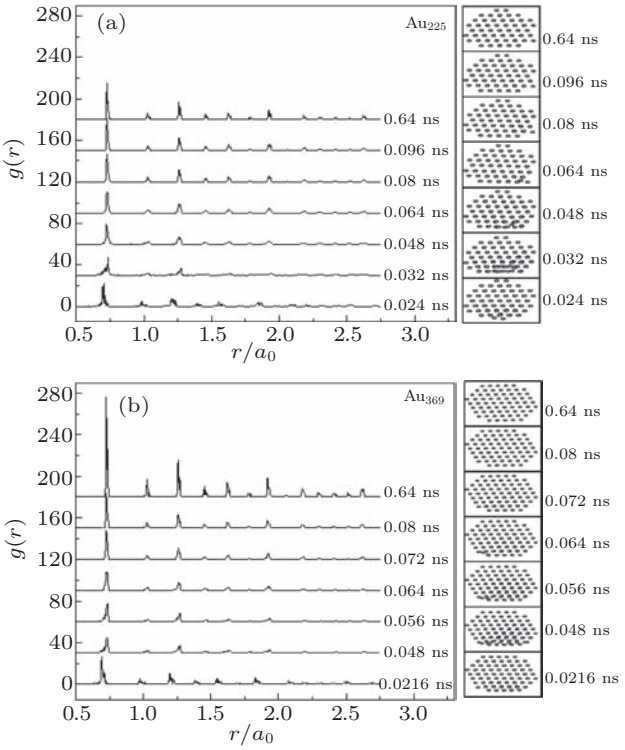


Fig. 2. The PDFs and corresponding atomic configurations at different times for (a) Au_{225} and (b) Au_{369} clusters.

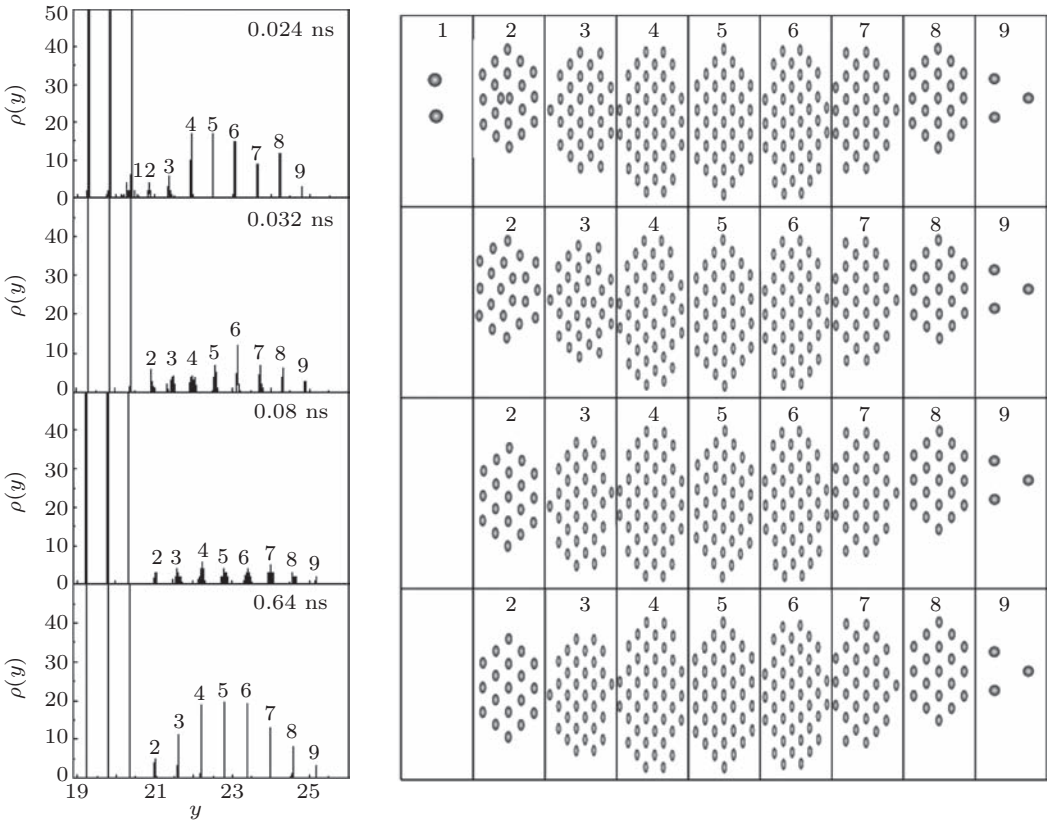


Fig. 3. The atom density profiles of Au_{225} clusters at different times and the corresponding local atom packings.

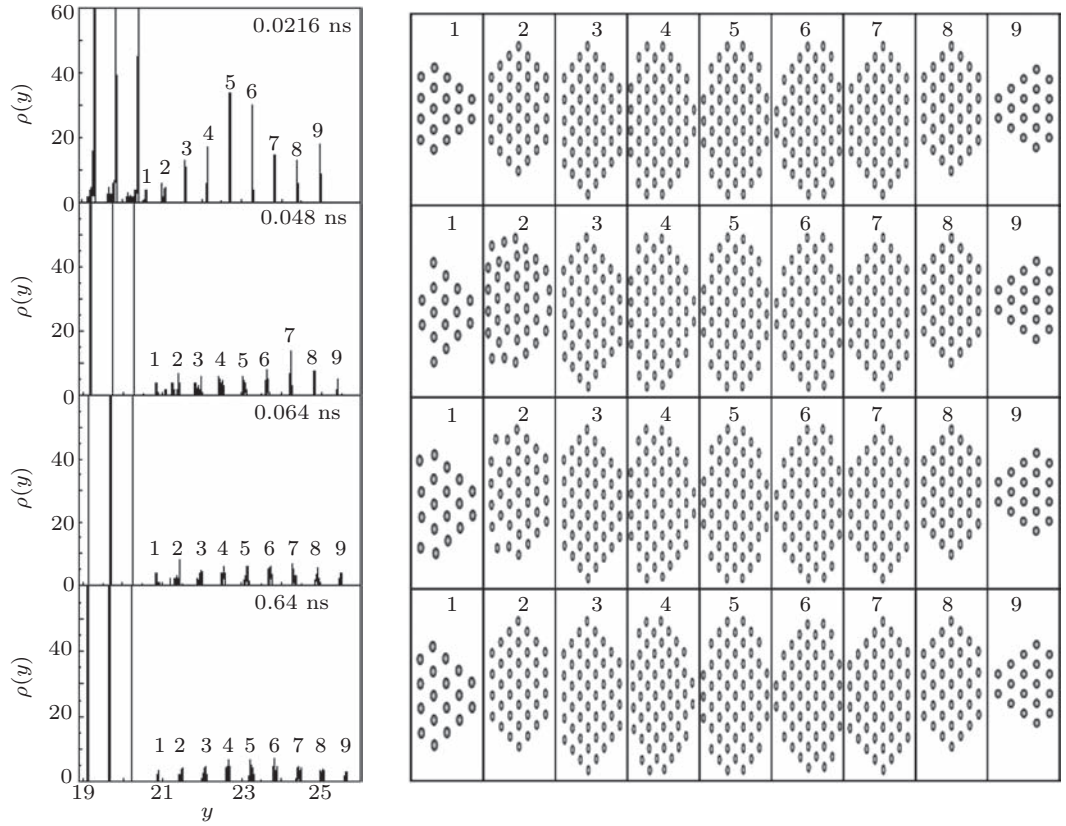


Fig. 4. The atom density profiles of Au_{369} clusters at different times and the corresponding local atom packings.

As shown in Fig. 3, at 0.024 ns there are some small peaks across the Au_{225}/MgO interface, implying that some atoms are distributed in these zones, which is due to the deformations occurring in the surface part of the MgO substrate and the supported cluster. At this time, two Au atoms are on the MgO surface, where they form the 1st layer shown in the atomic packing. The right atomic packing also shows that at this time, one Au atom moves from the first layer to the second layer, resulting in the changes of atomic positions in layers two and three. Meanwhile, in the upper layers there are some minor changes. As the interaction proceeds, the Au atoms move into the inner part of the Au cluster, i.e. one atom moves from the second layer into the third layer, and two atoms move from the first layer into the second layer. The deformation evolves into the inner part of the Au cluster, which can be clearly observed, especially in layers two and three (see Fig. 2). In the deformation process of the supported Au cluster and with the increase in atom distance, the distance between the supported cluster and the support surface becomes large. The support deformation disappears at 0.032 ns, as shown in the atomic packing and the atomic density profile. At the subsequent time, the adjustment of the atom position takes place mainly when two Au atoms enter into layer three and the three added atoms find their FCC lattice positions in the third layer. In the meantime, although the atom positions from the fourth layer to the ninth layer have not largely changed, these atoms vibrate around their crystal lattice positions, resulting in the decreased peak heights and the increased peak widths shown in the atomic density profiles. At 0.08 ns, an eight-row geometry with an *AB* atomic packing order constructed by 34 atoms is formed in the third layer, while 19 atoms construct the contact layer with the MgO surface marked as layer two. Afterwards, the Au atoms gradually stabilize at their lattice positions, and the atomic density profiles correspondingly present thin peaks.

At the beginning stage of the interaction between the Au_{369} cluster and the MgO surface (at 0.0218 ns), the deformation of the MgO surface and the contact part of the supported cluster can be observed in the atomic density profile, as shown in Fig. 4, where the Au cluster is composed of nine layers along the [010] direction. When the bottom of the supported Au_{369} cluster is some distance away from the MgO(010) surface, the support deformation disappears and the deformation mainly occurs in the supported cluster, as

shown in the atomic density profile at 0.048 ns, where layers one and two are almost connected. The phenomena are due to the fact that the two Au atoms in the first layer leave their initial positions and move close to the second layer, as shown in the atomic configuration. At this time, some of the atoms in the third to the eighth layer vibrate near their lattice positions. Hence, owing to the atomic packing changes, the peak height decreases and the width increases, implying that the atom distribution scope increases. With time increasing to 0.064 ns, the apparent position adjustment of the Au atoms can be found mainly in the two layers connected with the support surface, where the two atoms again move back into the first layer and a few of the atoms in the second layer are found to leave their original lattice point positions. Afterwards, the atoms gradually adjust their positions. At 0.64 ns, the cluster again becomes the FCC cluster but with a larger atom neighbor distance, as shown in the atomic packing.

4. Conclusion

In this work, MD simulations with the Long–Chen version of pair potential reveal the local structure changes of Au_{225} and Au_{369} clusters with their (111) facets supported by MgO(010) surfaces at low temperatures. The structural changes of these clusters clearly include an initial interaction stage, during which both the substrate and the supported cluster are deformed, followed by the detachments of the supported Au clusters from the substrate. In the subsequent stages, the atoms in the two clusters adjust their positions, although the final products have the FCC packing order of the atoms. The nearest neighbor distance between the atoms is adjusted to the MgO lattice constant, and the two supported clusters present different structural change processes and geometries. For the Au_{225} cluster with a small contact area of three atoms, during the structural change process the contacted three atoms move into the inner part of the supported cluster and the area contacting the support surface is composed of more atoms. For the Au_{369} cluster, its contact area is also enlarged after a stage where two atoms move between the two layers near the support surface, though the area includes the same number of Au atoms before and after being supported.

References

[1] Inntam C, Moskaleva L V, Neyman K M, Nasluzov V A and Rosch N 2006 *Appl. Phys.* A *Mater. Sci. Pro.* **82** 181

[2] Molina L M and Hammer B 2005 *Appl. Cataly.* A **291** 21

[3] Del Vitto A, Pacchioni G, Delbecq F O and Sautet P 2005 *J. Phys. Chem.* B **109** 8040

[4] Ricci D, Bongiorno A, Pacchioni G and Landman U 2006 *Phys. Rev. Lett.* **97** 036106

[5] Zimmerman R L, Ila D, Williams E K, Poker D B, Hensley D K, Klatt C and Kalbitzer S 1999 *Nucl. Instru. Meth. Phys. Res. Section* B **148** 1064

[6] Pauwels B, Van Tendeloo G, Bouwen W, Kuhn L T, Lievens P, Lei H and Hou M 2000 *Phys. Rev.* B **62** 10383

[7] Wang C M, Thevuthasan S, Shutthanandan V, Cavanagh A, Jiang W, Thomas L E and Weber W J 2003 *J. Appl. Phys.* **93** 6327

[8] Walter M and Hakkinen H 2005 *Phys. Rev.* B **72** 205440.

[9] Ma Y D, Dai Y, Wei W, Liu X H and Huang B B 2011 *J. Solid State Chem.* **184** 747

[10] Wei W, Dai Y, Guo M, Zhu Y T and Huang B B 2011 *J. Phys. Chem.* C **114** 10917

[11] Wei W, Dai Y, Lai K R, Guo M and Huang B B 2011 *Chem. Phys. Lett.* **510** 104

[12] Inntam C, Moskaleva L V, Yudanov I V, Neyman K M and Rosch N 2006 *Chem. Phys. Lett.* **417** 515

[13] Frondelius P, Hakkinen H and Honkala K 2007 *Phys. Rev.* B **76** 073406

[14] Fuente S A, Belelli P G, Ferullo R M and Castellani N J 2008 *Surf. Sci.* **602** 1669

[15] Kizuka T and Tanaka N 1997 *Surf. Sci.* **386** 249

[16] Zhang L, Li W and Wang S Q 2010 *Chin. Phys.* B **19** 073601

[17] Zhang L and Sun H X 2009 *Solid State Comm.* **149** 1722

[18] Shao C W, Wang Z H, Li Y N, Zhao Q and Zhang L 2011 *Acta Phys. Sin.* **60** 083602 (in Chinese)

[19] Song C F, Fan Q N, Li W, Liu Y L and Zhang L 2011 *Acta Phys. Sin.* **60** 063104 (in Chinese)

[20] Fan Q N, Li W and Zhang L 2010 *Acta Phys. Sin.* **59** 2428 (in Chinese)

[21] Zhang L, Zhang C B and Qi Y 2007 *Chin. Phys.* **16** 77

[22] Zhang L and Fan Q N 2011 *Physica Script* **84** 045303

[23] Zhang L and Li W 2012 *Comp. Mater. Sci.* **51** 91

[24] Xu S N, Zhang L, Qi Y and Zhang C B 2010 *Physica* B **405** 632

[25] Zhang L, Xu S N, Zhang C B and Qi Y 2009 *Comp. Mater. Sci.* **47** 162

[26] Hutchings G J, Brust M and Schmidbaur H 2008 *Chem. Soc. Rev.* **37** 1759

[27] Bracey C L, Ellis P R and Hutchings G J 2009 *Chem. Soc. Rev.* **38** 2231

[28] Zhang L and Wang S Q 2010 *J. Nanosci. Nanotech.* **10** S7820

[29] Long Y and Chen N X 2008 *Surf. Sci.* **602** 46

[30] Long Y and Chen N X 2008 *Surf. Sci.* **602** 1122

[31] Zhang L, Wang S Q and Ye H Q 2006 *Chin. Phys.* **15** 610